Gondwana Research 21 (2012) 4–18

Contents lists available at ScienceDirect

Gondwana Research

journal homepage: www.elsevier.com/locate/gr

GR Focus Review

Rheology of the continental lithosphere: Progress and new perspectives

Wang-Ping Chen [a,b,*], Shu-Huei Hung [c], Tai-Lin Tseng [c], Michael Brudzinski [d], Zhaohui Yang [e], Robert L. Nowack [f]

[a] Department of Geology, University of Illinois, Urbana, IL 61801, USA
[b] Department of Ocean Science and Engineering, Zhejiang University, Hangzhou, China
[c] Department of Geosciences, National Taiwan University, Taipei, Taiwan, ROC
[d] Department of Geology, Miami University, Oxford, OH, USA
[e] Department of Geological Sciences, University of Colorado, Boulder, CO, USA
[f] Department of Earth and Atmospheric Sciences, Purdue University, W. Lafayette, IN, USA

ARTICLE INFO

Article history:
Received 19 February 2011
Received in revised form 3 July 2011
Accepted 15 July 2011
Available online 23 July 2011

Keywords:
Rheology
Continental lithosphere
Jelly sandwich model
Focal depths
Tectonics
Greater India

ABSTRACT

While the surface of Tibet is undergoing pervasive pure shear, stable terranes, straddling subsurface sutures, remain in the sub-continental lithospheric mantle (SCLM), attesting to its strength. Furthermore, sub-horizontal, cohesive remnant of Indian SCLM is traced northward from the Himalayan deformation front for about 600 km, exemplifying the longevity of buoyant, strong SCLM of Archean shields. Bimodal distribution of earthquake depths, with peaks concentrating in the upper/middle crust and near the Moho, has been a longstanding evidence for strong SCLM. Recent results from the Himalayas—Tibet and along the East African rift system not only corroborate the bimodal distribution but also firmly established that large earthquakes occur below the Moho. Intriguingly, non-volcanic tremors—newly discovered mode of elastic strain release—also occur near the Moho but well below the seismogenic zone in the upper/middle crust. Considering recent field observations and laboratory experiments of viscosity contrast across the Moho, the SCLM must be strong enough to accumulate elastic strain, a prerequisite for earthquakes, over geological time. Moreover, under laboratory conditions, recent advances that link the termination of frictional instability, an analogue for earthquakes, and the onset of crystal plasticity, provided a physical basis for limiting temperatures of crustal (~300–400 °C) and mantle (~600–700 °C) earthquakes. While any single rheological model cannot possibly account for all tectonic settings (which also evolve with time), lithological contrast across the Moho is important in shaping the bimodal distribution of strength in the continental lithosphere.

Contents

1. Introduction . . . 5
2. New modes of fault slip: tremors and low-frequency earthquakes . . . 5
3. Distinct terranes of sub-continental lithospheric mantle and subsurface suture zone . . . 6
   3.1. Stable terranes attest to strength of the lithospheric mantle . . . 6
   3.2. The subsurface suture zone . . . 8
   3.3. The Greater Indian shield: longevity of lithospheric mantle . . . 9
4. Focal depths of intra-continental earthquakes . . . 9
   4.1. Background . . . 9
   4.2. Bimodal distribution of focal depths . . . 10
5. Field observations and simulations in the laboratory . . . 11
6. Discussions . . . 14
   6.1. Deep aftershocks . . . 14
   6.2. Stable terranes of SCML . . . 14
   6.3. Epilogue . . . 14
7. Concluding remarks . . . 15
Acknowledgements . . . 15
References . . . 15

* Corresponding author at: Department of Geology, University of Illinois, Urbana, IL 61801, USA. Tel.: +1 217 333 2744; fax: +1 217 244 4996.
E-mail address: wpchen@uiuc.edu (W.-P. Chen).

1342-937X/$ – see front matter © 2011 International Association for Gondwana Research. Published by Elsevier B.V. All rights reserved.
doi:10.1016/j.gr.2011.07.013

1. Introduction

2010 marks the centennial of the discovery of the Mohorovičić discontinuity (Moho), the boundary between the Earth's crust and the mantle where major contrasts in seismic wave speeds and density occur. These contrasts are a consequence of a strong lithological difference across the Moho, which is also a key factor for rheology: under similar laboratory conditions, ultramafic rocks of the mantle typically have higher yield stress than less mafic rocks of the crust (e.g., Goetze, 1978). Rheological contrast across the Moho is particularly important for the continental lithosphere where considerable thickness of the crust places this important boundary at significant depth within the lithosphere.

Extrapolating results from experimental rock physics, over orders of magnitudes in scale and in strain rate, lead to a bimodal distribution of shear stress ("the strength-envelope") in the continental lithosphere. In the upper crust, brittle behavior, such as frictional sliding and fracturing, dominates. These processes are very sensitive to effective pressure (the difference between ambient and pore pressure) but not to temperature, leading to a linear increase in lithospheric strength as a function of depth (Byerlee's rule, Fig. 1). In the mid- to lower crust, increasing temperature promotes plastic micro-mechanisms such as dislocation creep that would relax build up of high stresses. Plastic mechanisms generally follow the Arrhenius relationship so the strength should drop exponentially with increasing temperature at depth, leading to a peak in strength near the mid-crust near where the transition between brittle and plastic deformation ("brittle–ductile transition") takes place.

The trend of rapidly decreasing strength reverses itself near the Moho because of the major change from crustal lithology to ultramafic assemblages of the mantle, and a second peak in strength is expected in the uppermost mantle near the Moho (Fig. 1). At even greater depths, the ductile strength of ultramfic materials diminishes at high temperature, making a gradual transition into the asthenosphere. For the plastic regime, the upper limit of stress accumulation also depends on strain rate which, for simplicity, is assumed to be constant and at steady state in Fig. 1. In general, a higher strain rate will allow more stress to accumulate in the lithosphere (e.g., see a recent review by S.-I. Karato (2010) and references therein). Furthermore, strain rate may vary as a function of depth. For instance, a zone of concentrated shear in the lower crust will smooth out the abruptness of increase in shear stress near the Moho.

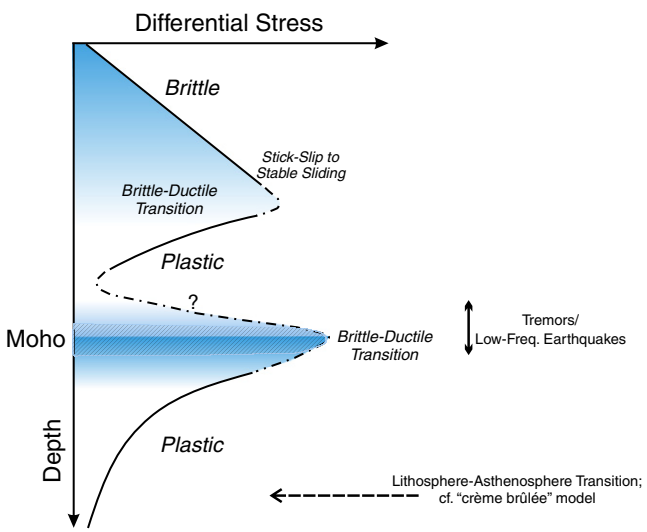

Fig. 1. A schematic diagram showing how limiting values of shear stress vary with depth in the continental lithosphere (the "jelly sandwich" model). Seismogenic regions are shaded in blue while the Moho transition is hatched. Stress in the brittle regime is controlled by a linear relationship between shear and normal stresses (Byerlee's rule), while that in the plastic regime is mainly determined by distinct flow laws for crust and mantle materials (Chen and Molnar, 1983; Chen and Kao, 1996). For the latter regime, the upper limit of stress accumulation also depends on strain rate which, for simplicity, is assumed to be constant in the diagram. Data presented by Chen and Yang (2004) and Yang and Chen (2010) showed that sub-crustal earthquakes as large as magnitude 6 occurred below the Moho. New modes of strain release, in the form of non-volcanic tremors and low-frequency earthquakes, also occur near the second peak of conventional earthquake activities (Ohmi et al., 2004; Shelly and Hardebeck, 2010). In comparison, the so-called "crème brûlée" model effectively places the lithosphere–asthenosphere transition above the Moho.

Chen et al. (1981) provided the first evidence that the so-called "jelly sandwich" rheology is indeed applicable to the real Earth, showing that sub-crustal earthquakes as deep as 90 km occur beneath southern Tibet where crustal earthquakes concentrate between depths of only 5 and 15 km. Earthquakes are associated with sudden release of accumulated elastic strain. As such, a seismogenic zone must be strong enough to allow elastic strain to accumulate and brittle deformation to occur—otherwise plastic flow would prohibit the accumulation of elastic stress. Moreover, frictional instability, the analogue of seismogenesis in laboratory experiments, terminates at high temperatures near the onset of significant plasticity (Brace and Byerlee, 1970; Stesky et al., 1974; Blanpied et al., 1991; Scholz, 1998; Boettcher et al., 2007; also see Section 4.1), so the seismic to aseismic transition is closely linked with the changeover from brittle to plastic deformation where peaks in the strength profile are expected (Fig. 1).

Subsequently, Chen and Molnar (1983) carried out a global study to show that the distribution of earthquake focal depths are bimodal in several intra-continental regions, with peaks in the upper to mid-crust and near the uppermost mantle, respectively (to be precise, the level of seismicity refers to the amount of elastic strain being released by earthquakes; see later discussions of Fig. 5 in Section 4.2). Of course, seismicity cannot directly address the strength of the aseismic lower crust in these regions.

In the past decade, rheology of the continental lithosphere has been revisited by several studies. Based on modeling of gravity data, McKenzie and Fairhead (1997) reported a small effective elastic thickness (*Te*) in Africa. Even though *Te* is a mathematical parameter whose physical meaning in irreversibly deformed materials is not defined, those authors inferred that strength of the lithosphere resides mainly in the crust. In effect, this so-called "crème brûlée" model places the bottom of the lithosphere or the top of the asthenosphere above the Moho.

In terms of field observations, Austrheim and Boundy (1994) and Jackson (2002) used pseudotachylites in mafic granulites to argue for a strong lower crust. Notice that this view goes beyond just attributing most of the lithospheric strength to reside somewhere in the crust, it specifically calls for high strength in the lower crust. We shall revisit this particular subject later in this article. Suffice it to say that studying pseudotachylites in the lower crust alone does not address the key question of whether the uppermost mantle is strong.

In this article, we summarize some recent progress on rheology of the continental lithosphere. More fundamentally, we address this topic from perspectives that are either entirely new or those that merit further clarifications and discussions. We shall begin our discussion with new modes of fault slip that are distinct from conventional earthquakes, followed by the longevity of distinct terranes of the lithospheric mantle, and finally recent results of (conventional) earthquake focal depths.

2. New modes of fault slip: tremors and low-frequency earthquakes

In the past few years, evidence has been rapidly accumulating that fault slip occurs over a wide range of characteristic time-scales that are distinct from ordinary earthquakes and continuous fault slip. The latter two phenomena represent only the ends of a broad spectrum of fault slips. The new modes of fault slip bear many different names and there is no consensus on mechanisms that control this wide array of behaviors. What seems clear is that for a given seismic moment, such new modes of slip have characteristic durations that are greater than

conventional earthquakes (Ide et al., 2007 and references therein). Ide et al. (2007) collectively referred to these slip events as "slow earthquakes". While the difference between conventional and slow earthquakes seems convincing, data for non-traditional earthquakes are limited. Furthermore, large scatter in the data make it unclear if all slow events follow a single scaling rule. (The seismic moment M, is a true measure of the size of a slip event, defined by the product of the slip area (A), the amount of slip (D) and the shear modulus of the source region (μ) (Aki and Richards, 2002). In light of the prevalence of unconventional earthquakes, we propose that the term be generalized to "slip moment".)

Most of these new models of strain release occur along or near the plate interface at subduction zones where significant vertical motions across the plate boundary make it difficult to investigate the role of lithological control over rheology. A notable exception is the segment of the San Andreas transform fault system near Parkfield, California where strike-slip motion dominates. The Parkfield region is well known for several intriguing phenomena. First, it is at the transitional junction of a continually creeping, largely aseismic segment of the fault and a segment that is currently "locked", but repeatedly ruptured by large earthquakes in the past (e.g., Sieh, 1978; Savage, 1993). Second, with the notable exception of the earthquake in 2004, moderate-sized earthquakes seem to have recurred at an interval of about 22 years (e.g., Savage, 1993; Bakun et al., 2005). Third, repeating earthquakes, events that recur at specific patches of the fault, are common (e.g., Nadeau and Johnson, 1998).

In 2005, Nadeau and Dolenc reported tectonic (non-volcanic) tremors—low amplitude but long-lasting vibrations—in the Parkfield area. Recently, Shelly and Hardebeck (2010 and references therein) showed that these tectonic tremors appear to be comprised of numerous overlapping low-frequency earthquakes: events with distinct P- and S-wave arrivals but whose frequency-content is only slightly lower than ordinary earthquakes of comparable slip moments. In all, Shelly and Hardebeck (2010) relocated 88 families (or spatial clusters) of tremors that span a distance of about 150 km along the San Andreas fault near Parkfield (Fig. 2). In a sequence of publications, Shelly (2010a, 2010b) also described in detail intriguing correlations between tremor activities and larger earthquakes, such as the Parkfield earthquake of 2004. For the purpose at hand, the most important observation is that the tremor families all occurred between depths of about 18 and 30 km, significantly below the zone of ordinary micro-earthquakes and the slip zone during the 2004 Parkfield earthquake that concentrated above depths of 10 to 15 km in the upper crust (Fig. 2).

Precise position of the Moho is not known along this section of the San Andreas fault. Based on seismic reflection, a technique not particularly suitable for determining precise depths of deep interfaces, recent results of Bleibinhaus et al. (2007) did not provide much constraint on the Moho. Using a short profile (22 km in length) perpendicular to the fault zone, an earlier image by McBride and Brown (1986) was also noisy. After heavy processing, they reported a collection of discontinuous reflectors just after 8 s in two-way travel-time and interpreted them as the Moho at depths of about 25 km and 29 km beneath the Salinian block on the southwestern side and the Franciscan terrane on the northeastern side of the fault, respectively. These values are consistent with seismic refraction data re-assessed by Walter and Mooney (1982). Result for the Salinian block is recently corroborated by Ozacar and Zandt (2009) who used crustal receiver-functions derived from one broadband station PKD close to the town of Parkfield.

For ready comparison, we mark the range of estimated Moho depths in Fig. 2. Shelly and Hardebeck (2010) inferred that all tremor families are in the lower curst. However, given the range of about 10 km in the depths of such events and uncertainties in estimated positions of the Moho, many tremors occurred very close to the Moho and some of them may have occurred in the uppermost mantle, resembling the position of unusually deep earthquakes that occur near and below the Moho in a number of regions elsewhere (Fig. 1; see further discussions and references in Section 4.)

At any rate, two observations are clear: 1) the majority of tremor families occur close to the crust–mantle transition; and 2) along most of the fault, there is a pronounced gap of 10 km or more between the zone of upper/middle crustal earthquakes and tremors (Fig. 2). The latter result is robust regardless of the exact configuration of the Moho. Another example of these patterns along strike-slip fault zones is associated with the Western Tottori earthquake of 2000 in southwestern Japan where the position of the Moho near the source region is unknown (Ohmi et al., 2004). In this case, both the main shock and most aftershocks occur in the top 12 km of the crust. A number of low-frequency earthquakes occurred between depths of 25 and 35 km both prior to and after the main shock, leaving a conspicuous, aseismic gap between depths of 12 and 25 km. At this juncture, the dynamics of tremor activity and low-frequency earthquakes and physical conditions that govern their genesis are not known and remain as targets of intense research (http://www.earthscope.org/institutes/spectrum_fault_slip_behaviors). Nonetheless, such events do release seismic radiation and therefore require some degree of elastic strain accumulation. As such, the most straightforward interpretation is that the gap in seismic radiation corresponds to a minimum in crustal strength where little or no elastic stress can accumulate.

3. Distinct terranes of sub-continental lithospheric mantle and subsurface suture zone

3.1. Stable terranes attest to strength of the lithospheric mantle

Since the advent of broadband, digital seismometry, seismology has made great strides in several fronts. For instance, observations over a broadband of frequencies translate into high resolution in the time-domain. This advance greatly facilitates understanding of the seismic wavefield which, in turn, results in highly precise

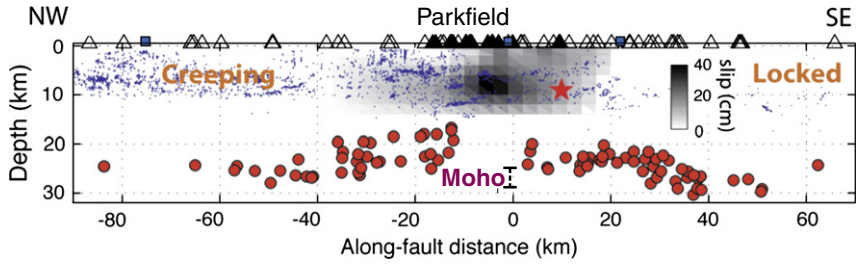

Fig. 2. Cross-section of tremor family locations (red circles) near the Parkfield section of the San Andreas fault zone (taken from Shelly and Hardebeck (2010)). For comparison, we add estimated positions of the Moho ("I"-beam symbol) by McBride and Brown (1986), Ozacar and Zandt (2009), and Walter and Mooney (1982). Blue dots show relocated micro-seismicity within 5 km of the fault trace from 1984 to 2003 (Waldhauser and Schaff, 2008). Red star indicates hypocenter of the M ~6 earthquake in 2004, with gray shading showing the co-seismic and first 230 days of post-seismic slip (Murray and Langbein, 2006).

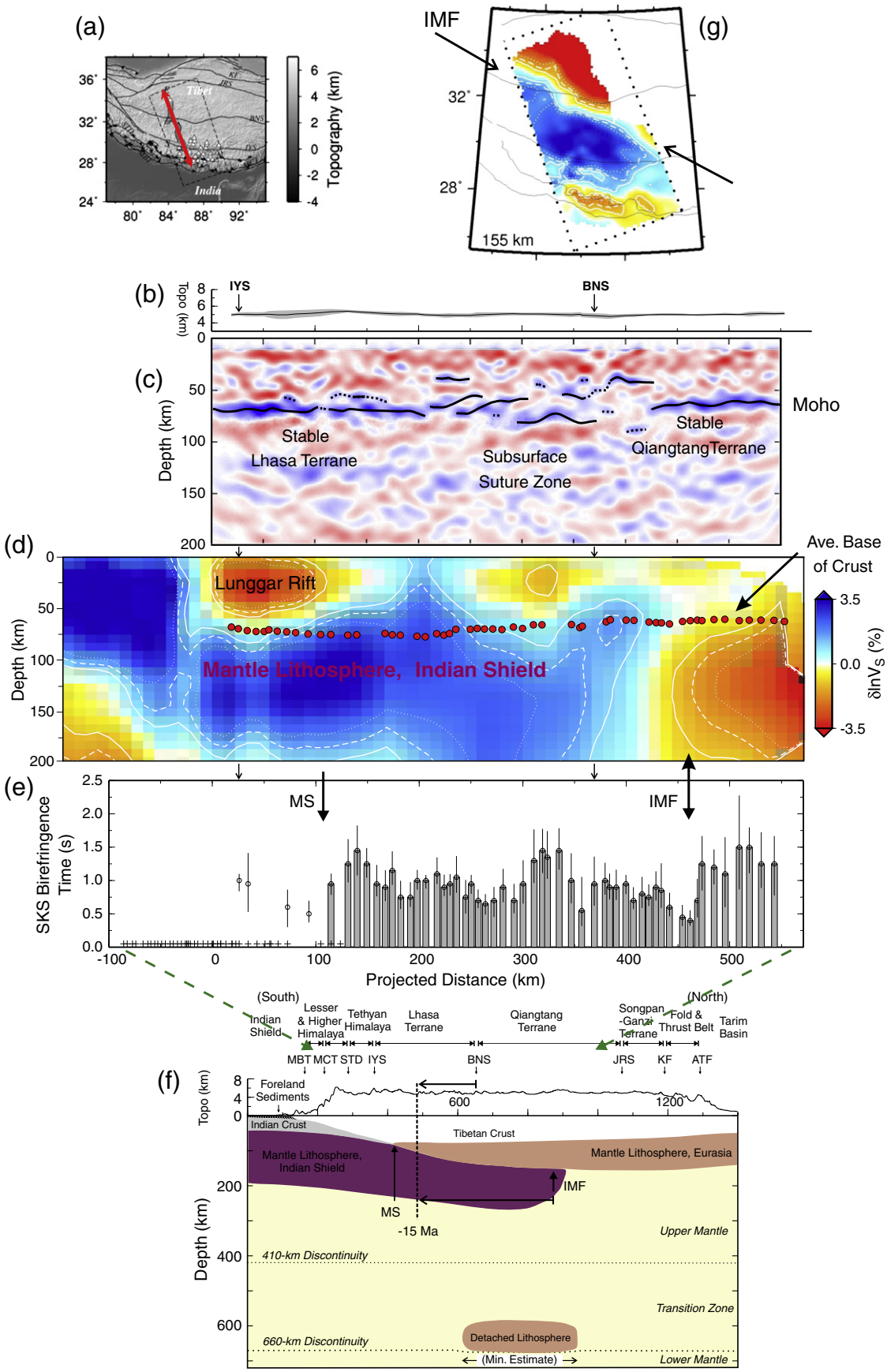

determination of seismic properties at depth, including but not limited to sharper images of structures in the subsurface. Also advances in micro-electronics allow large-scale field deployments with sufficient station density to reduce the ever present problem of spatial aliasing. Finally, rapid expansion of computing power makes it possible to analyze vast amounts of seismic data in a timely fashion.

In sum, these advances afford yet another new perspective to study rheology by examining how continents respond to deformation over lithospheric scales at depth. Fig. 3 summarizes the most salient results of Project Hi-CLIMB (*H*imalayan–*T*ibetan *C*ontinental *Li*thosphere during *M*ountain *B*uilding) (Chen et al., 2010). The mainstay of Hi-CLIMB is a combined linear and regional broadband seismic array that covers an L-shaped region of about 800 km by 500 km over the most prominent case of active continental collision—the Himalayan–Tibetan orogen.

There is a consensus that this orogen is a consequence of ongoing convergence, which initiated in the Eocene, between the northern Indian shield and the Lhasa terrane of southern Tibet. On the surface, the Indus–Yarlung suture (IYS) marks the boundary between these two terranes. Farther northward, another collision originated in late Jurassic to early Cretaceous between the Lhasa terrane and the Qiangtang terrane in central Tibet and the corresponding surficial suture is the Bangong–Nujiang suture (BNS) (e.g., Yin and Harrison, 2000).

With a new technique of constructing deep-penetrating, virtual seismic reflection profiles from earthquakes, Tseng et al. (2009) precisely determined the average thickness of crust beneath Tibet over a distance of more than 500 km (Fig. 3d). Along the southern part of the Lhasa terrane, the crust reaches a great thickness of almost 75 km. Starting near the northern portion of the terrane, the crust gradually thins northward to just over 60 km below the central Qaingtang terrane.

More importantly, Nowack et al. (2010) applied a newly developed method of seismic migration to obtain multi-frequency, high resolution images of the Moho and the lower crust along the same profile of Tseng et al. (2009). This migration scheme expands scattered seismic wavefield observed on the surface as a collection of Gaussian beams and requires no *a priori* smoothing of either the input seismograms or the resulting images. Furthermore, no special treatment is required to handle juxtaposition of materials of different seismic impedance resulting from complex geological structures (cf. Bostock et al., 2001). Starting with converted shear-waves from planar, incident *P*-waves (the often used *Ps* phase in so-called crustal receiver-functions), Gaussian beam migration revealed that in spite of repeated events of continental collision, the Moho remains a sharp interface without major undulation or obvious interruption over distances of about 200 km near both ends of the profile (Fig. 3c). Using the configuration of the Moho as a strain marker, we identify sharp, flat-lying portions of the Moho toward the southern and northern ends of the cross-section as stable portions of the sub-continental lithospheric mantle (SCLM) under Lhasa and Qiangtang terranes, respectively.

This result is particularly noteworthy in that we applied no lateral smoothing that emphasizes sub-horizontal features. Moreover, numerous modern geodetic data (based on GPS) on the surface indicate that the upper crust of Tibet, when measured at scales above the order of 10 km, is predominantly under uniform pure shear strain (e.g., Chen et al., 2004; Zhang et al., 2004; Meade, 2007; Thatcher, 2007). In contrast, disturbance of the Moho, intriguing in its nature and significant in its own right (Tseng et al., 2009; Nowack et al., 2010; and discussions to follow), is limited to a subsurface suture zone in the central portion of the profile that marks the subsurface join between opposing, stable terranes.

The existence of distinct terranes of the SCLM, over distances of hundreds of kilometers with little signs of deformation, indicates that the SCLM under Tibet is strong enough to sustain ongoing convergence and repeated collision over geologic time. Our conclusion is independently supported by observations of Moho offsets that remain abrupt over hundreds of millions of years in other collisional orogens (e.g., Marillier et al., 1989; Goleby et al., 1998) and by numerical simulations (e.g., Watts and Burov, 2003; Burov and Watts, 2006, and references therein). These results of thermo-mechanical modeling showed that unless the upper mantle beneath continents has considerable mechanical strength and is an integral part of the lithosphere, some of the most important geological processes that have clearly repeated over geological time, such as subduction, orogeny, and rifting, cannot operate over geological time-scales. It has also been proposed that strong SCLM is essential for the super-continent cycles to operate (e.g., Santosh et al., 2009).

3.2. The subsurface suture zone

In Fig. 3c, throughout the middle one-third of the profile, the Moho is laterally disrupted in many places and vertically dispersed over depths as shallow as 40 km and as deep as 80 km. Such subsurface suture zones that join stable mantle terranes have been noted before from the interpretation of conventional seismic profiles (e.g., Marillier et al., 1989), but not over such a wide distance laterally (over 200 km), or

Fig. 3. Maps and north–south trending profiles across southern and central Tibet, summarizing key results from Project Hi-CLIMB. (a) A map showing locations of seismic stations (triangles) and the region being investigated (box outlined by dashed lines). The red solid line indicates the location of profile along which an image of $\delta \ln V_S$ is shown in (d). Other features are major geologic boundaries (solid curves), including (from north to south) KF, the Kunlun Fault; JRS, the Jinsha River Suture; BNS, the Bangong–Nujiang Suture; IYS, the Indus–Yarlung Suture; STD, the South Tibet Detachment System; MCT, the Main Central Thrust; and MBT, the Main Boundary Thrust. (b) A cross-section showing mean elevation (solid curve) and its standard deviation (gray shading) across a swath of about 200 km in width, or the approximate separation between each virtual seismic source and station for the *SsPmp* phase (see (d)), along the profile. (c) Cross-sections of the Tibetan lithosphere as imaged by Gaussian beam migration of direct *P*- to *S*-wave conversions. The convention is that a scatterer representing an increase in impedance with depth results in a blue pixel centered on the position of the scatterer. Our interpretation of the Moho is highlighted by black curves (dashed when uncertain). Notice smooth-varying, near-horizontal Moho at both ends of the profile, marking stable—thus strong—lithospheric mantle blocks that remain intact through continental collisions. The sub-surface suture zone is the join between the two stable terranes. (d) Estimated crustal thickness (red dots) based on the differential timing between seismic phases *SsPmp* and *Ss* ($T_{SsPmp-Ss}$; see Tseng et al. (2009) for explanations of the technique and details of analysis), and average *P*-wave speed in the crust (V_P), including perturbations to a background values of 6.30 km/s as determined from travel-time tomography). Superimposed is a long cross-section of $\delta \ln V_S$ from multi-scale, finite-frequency travel-time tomography (Hung et al., 2010, 2011). IMF marks the Indian mantle front where lateral variations in V_S is most pronounced (see contours; solid, dashed, and dotted contours correspond to $\pm 1\%$, $\pm 1.5\%$, and $\pm 2\%$ of anomalies, respectively.) Notice the pronounced anomaly of high V_S at the southern end of the profile where the northern Indian shield is yet to be involved in the orogeny. This feature then dips southward and becomes sub-horizontal under Tibet (also see map-view shown in (g)). This feature is interpreted as underthrust Indian mantle lithosphere of Archean age, thus being chemically depleted and buoyant. In the image, we masked out portions of the models where sampling is sparse and resolution is poor (Hung et al., 2010, 2011). (e) A profile of *S*-wave birefringence across Tibet. MS marks the mantle suture or the southern limit of the Tibetan lithospheric mantle. Open circles are isolated cases of birefringence south of the mantle suture. Measurements are shown with error-bars except null birefringence observed along the southern portion of the cross-section (crosses). IMF can be consistently traced across two other profiles for about 600 km farther to the east (Chen and Özalaybey, 1998; Chen et al., 2010). (f) A schematic cross-section showing the current configuration of the sub-continental lithospheric mantle, including a large-scale anomaly of high *P*-wave speed resting on top of the lower mantle and interpreted as the remnant of thickened (and subsequently detached due to Rayleigh–Taylor instability) lithospheric mantle (Chen and Tseng, 2007). The dimension of the detached lithosphere shown is a minimal estimate, limited by current coverage of seismic arrays around Tibet. The dashed vertical line show reconstructed positions of the IMF and the BNS and they nearly coincide at 15 Ma ago, at the onset of the Rayleigh–Taylor instability. For reference, we also label key geologic units/boundaries and topography at the present (vertically exaggerated by a factor of 13.15). (g) An image (in map-view) of $\delta \ln V_S$ beneath central Tibet, at a depth of 155 km, from multi-scale, finite-frequency travel-time tomography. Solid curves show major geologic boundaries as those in (a). See (d) for explanations of contours and labels. Notice the slab-like anomaly of high V_S in the center of the image (also see cross-section shown in (d)), interpreted as underthrust Indian mantle lithosphere of Archean age (Greater India).

involving complex, strong lower to mid-crustal reflectors/scatterers across which the contrast of seismic impedance approaches that of the Moho (Fig. 3c). Nonetheless, these results are robust, as demonstrated not only by careful tests of Gaussian beam migration using synthetic receiver-functions but also by modeling of the coda of *S*-wave forms (Tseng et al., 2009; Nowack et al., 2010).

Another piece of independent evidence comes from field observations of exhumed orogens where mid- to lower crust is now exposed on the surface. For instance, in the Western Gneiss region of Norway, numerous bodies of peridotite have been documented (e.g., Brueckner and van Roermund, 2004; Vrijmoed et al., 2008). Typically these bodies are surrounded by felsic gneiss associated with the Caledonian orogeny in the early Paleozoic and the degree of contrast in lithology exposed at surface is the same as that across the Moho. Given the fact that the Moho of the Western Gneiss region is currently at a depth of about 35 km below these outcrops (Artemieva and Thybo, 2008), there is little doubt that during the peak of the Caledonian orogeny, the peridotite bodies were at depths comparable to ultramafic scatterers in the Tibetan crust as imaged and modeled by high resolution seismic data (Fig. 3c). Because high resolution travel-time tomography of both *P*- and *S*-waves shows no significant anomalies along the subsurface suture zone (Hung et al., 2010, 2011), Nowack et al. (2010) interpreted that the incorporation of mafic or ultramafic materials into the lower crust is mainly a mechanical processes; but details on the origin and the evolution of such complex subsurface suture zones are not yet known.

3.3. The Greater Indian shield: longevity of lithospheric mantle

At even greater depths, an innovative inversion method that combines a data-adaptive, multi-scale expansion of model parameters and finite-frequency theory for wavefront-healing yields sharp images of travel-time tomography from data collected during Project Hi-CLIMB (Hung et al., 2010, 2011) (Fig. 3d and g). In a nutshell, this new method involves no *a priori* smoothing in any direction; and places small-scale features in the resulting images, only if the data have the resolution to require such features. At the longest wavelength, a changeover from high to low *P*- and *S*-wave speeds (V_P and V_S, respectively) near the northern end of the profile is readily apparent. As more details are added to improve the agreement between observed and predicted travel-times, a slab-like, sub-horizontal feature of high V_P and V_S, can be traced northward for about 600 km (Fig. 3d and g) (Hung et al., 2010, 2011). On the southern end of the profile, this key feature coincides with intact Indian shield in the foreland of the Himalayan–Tibetan orogen, and then it gradually dips to reach a maximum depth of about 250 km, and continues northward sub-horizontally beyond the surficial BNS (Fig. 3d).

A critical contribution of the new tomographic images lies in their regional coverage—a direct consequence of high-quality data from both a north–south trending, dense linear array and a regional network that operated concurrently during Hi-CLIMB. Fig. 3g shows a map-view of fractional changes in V_S at a depth of 155 km, near the center of the slab-like anomaly. Clearly this is a continuous feature with a lateral (east–west) extent of over 500 km, the limit of effective data coverage. Several additional pieces of independent evidence support the notion that the leading edge of northward underthrusting Indian SCLM (the Indian mantle front, IMF) reaches beyond the BNS in places.

Fig. 3e shows how the magnitude of transverse seismic anisotropy (birefringence), as measured by near-vertically incident *S*-waves (the *SKS* phase), varies along the profile. Position of the IMF, as indicated by strong, north–south variations in V_P and V_S, practically coincide with a marked increase in *S*-wave birefringence (Fig. 3e) (Chen et al., 2010). Inefficient propagation of head-waves in the uppermost mantle (Beghoul et al., 1993), large *S*–*P* travel-time residuals observed at teleseismic distances (Molnar and Chen, 1984), and deviation from crustal isostasy (Owens and Zandt, 1997; Tseng et al., 2009) all point to an unusually warm upper mantle beyond the IMF. High temperatures, also consistent with low V_P and V_S, and occurrences of recent volcanism (Chung et al., 2005; Hung et al., 2010, 2011), combined with continual northward advance of the IMF, form a condition conducive to E–W ductile flow which, in turn, probably contributed to large values of *S*-wave birefringence (Owens and Zandt, 1997; Jimenez-Munt et al., 2008).

Lateral continuity of the IMF as an important geodynamic demarcation include modeling of Bouguer gravity anomalies through plate flexure (Jin et al., 1996) and patterns of *S*-wave birefringence along two other profiles over a lateral distance of about 800 km (Chen et al., 2010 and references therein). Moreover, dynamic considerations also favor the interpretation that the slab-like, sub-horizontal anomaly of high V_P and V_S mark the trajectory of northward advancing Indian SCLM or the so-called "Greater India": the Indian shield, like most other shield regions, is likely to have a chemically refractory mantle lithosphere that provides the necessary buoyancy to counteract thermal contraction caused by more than 2.5 Ga of cooling since the Archean (e.g., Jordan, 1978, 1988). Near-neutral buoyancy of the Indian SCLM provides a ready explanation for the sub-horizontal configuration of northward advancing Greater India, otherwise a very cold, therefore dense, remnant of cratonic SCLM should plunge to depth.

Lately, Hung et al. (2011) further analyzed Hi-CLIMB data to obtain not only reliable, 3-D images of $\delta\ln V_P$ and $\delta\ln V_S$ (or fractional changes in V_P and V_S, respectively), but also that of $\delta\ln(V_P/V_S)$. To a large extent, the slab-like anomaly of high V_P and V_S in the upper mantle is associated with low V_P/V_S. Indeed Lee (2003) suggested that there is a negative correlation between the magnesium number (Mg#) and V_P/V_S; so one expects high Mg# for the Greater India, indicating depleted mantle materials whose V_P/V_S is low. Furthermore, the negative anomaly of $\delta\ln(V_P/V_S)$ is apparently restricted to depths no deeper than 200 km, somewhat shallower than the corresponding positive anomalies of V_P and V_S. This result is consistent with the isopycnic hypothesis (e.g., Jordan, 1978, 1988) that predicts that extraction of basalt in the Archean would have left the mantle lithosphere to be most depleted near its top. However, some recent studies questioned if the relationship proposed by Lee (2003), an extrapolation based on data measured at standard temperature and pressure, may be too strong (Faul and Jackson, 2005; Wagner et al., 2008). So a precise, quantitative relationship awaits more measurements under high pressures and temperatures.

Results of numerical simulations showed that compositional buoyancy alone seems insufficient to counteract convective instability expected along edges of cratonic roots where large lateral thermal gradient is expected. In addition, the cratonic SCLM must have sufficiently high viscosity. For dislocation creep, the estimated activation energy to maintain high enough viscosity is only about one-third of that for dry olivine (Shapiro et al., 1999a). S. Karato (2010) suggested that high degrees of basalt extraction left a particularly dry and strong cratonic root. Notice that while numerical simulations suggested that very high viscosity alone may be sufficient to explain the longevity of cratonic roots, compositional buoyancy is still necessary to account for a negligible cratonic signature in the geoid (Shapiro et al., 1999b).

In any event, the latest results based on high-quality seismic data indicate that continental collision does not destroy cratonic mantle lithosphere. Instead, the Greater Indian shield has advanced sub-horizonatlly northward by some 600 km beyond the collisional front and we attribute this remarkable configuration of overlapping lithosphere to compositional buoyancy and high strength of depleted Archean SCLM.

4. Focal depths of intra-continental earthquakes

4.1. Background

Before we summarize some important new results on the distribution of focal depths of intra-continental earthquakes, it is critical to emphasize that rheology of the lithosphere—a complex, multi-component system—depends on many factors, including temperature,

strain rate, bulk composition and mineral assemblages, grain size, the presence of fluids or volatiles, and crustal thickness. (A vast body of work has been carried out on these topics under laboratory conditions. For instance, see summaries by Evans and Kohlstedt (1995), Hirth and Kohlstedt (2003), S.-I. Karato (2010), Poirier (1995), and references therein.) As such, and considering the diversity and complexity of the continental lithosphere, no one model fits all tectonic settings or all stages of thermal evolution for a given setting. This all important point was made clear in earlier, global studies of the problem but not always enunciated in recent discussions.

Next we address the link between earthquakes and the strength profile (Fig. 1). Based on results from laboratory experiments, earthquakes are associated with the so-called stick-slip phenomenon in the frictional regime of brittle deformation (e.g., see Tse and Rice (1986) and the reviews by Scholz (1990, 1998)). Long intervals of "stick" correspond to seismic quiescence of the inter-seismic stage, while sudden slips of faults result in seismic events. Since the mid-1980s, there is a consensus that frictional instability can be conveniently described by a rate and state variable (the "Dieterich-Ruina") relationship. In its simplest form of one state variable, the coefficient of friction, μ, or the ratio between shear stress and effective normal stress is expressed as:

$$\mu = \mu_o + a\ \ln(V/V_o) + b\ \ln(\theta\ V_o/L), \tag{1}$$

where V is the sliding velocity, V_o a reference sliding velocity, μ_o the steady state friction at V_o, a and b are empirically determined properties of the material. L is a characteristic slip distance over which the system evolves to a new steady state; and θ, the state variable, evolves as follows:

$$d\theta/dt = 1 - \theta V/L. \tag{2}$$

An important point to note is that the combined parameter, $(a-b)$, is related to steady state friction, μ^{ss}, through

$$(a-b) = d\mu^{ss}/d(\ln V). \tag{3}$$

Furthermore, stability analyses showed that when $(a-b)$ is negative ("velocity weakening"; Eq. (3)), the system is unstable, leading to sudden slips or earthquakes (e.g., Tse and Rice, 1986). Thus seismic to aseismic transition at depth corresponds to the changeover from stick-slip to stable sliding.

The connection between seismic to aseismic transition and regimes of plastic deformation, depicted in Fig. 1, is through a strong dependence of $(a-b)$ on temperature. Using results from Blanpied et al. (1991) and Stesky et al. (1974), Scholz (1998) showed that for granite, a material well-studied in the laboratory and abundant in the upper crust of the Earth, $(a-b)$ is negative at low temperatures but becomes positive above about 350 °C. This limiting temperature for crustal seismicity is close to the onset of plasticity in quartz, an abundant, most ductile rock-forming mineral in granite (e.g., Brace and Byerlee, 1970; Scholz, 1998). In other words, through the limiting temperature, the onset of crystal plasticity greatly influenced the combined parameter $(a-b)$; so the seismic to aseismic transition is closely linked with the brittle–ductile transition where the first peak in the strength profile is expected (Fig. 1).

Recognizing that temperature is a key controlling factor for seismicity, it is heuristic to briefly review related issues of the oceanic lithosphere, whose thermal state is mainly a function of its age (Parsons and Sclater, 1977). Both Chen and Molnar (1983) and Wiens and Stein (1983) showed that globally, the limiting temperature for mantle earthquakes essentially follows the 700 ± 100 °C isotherm. These results have been corroborated by more recent work of McKenzie et al. (2005) who reevaluated thermal models and reported a slightly lower limit of about 600 °C (although some seismicity occurred above about 700 °C). In addition, Watts et al. (1980) also showed that the apparent thickness of the oceanic lithosphere, when measured by different indicators, increases with decreasing characteristic time-scale of loading (or equivalently increasing strain rate).

It is important to note that a limiting temperature of about 600–700 °C for mantle earthquakes is consistent with where $(a-b)$ changes sign (from negative to positive at higher temperatures) for the most abundant mineral in the mantle, olivine, when experimental results by Boettcher et al. (2007) are extrapolated to geological strain rates. Therefore, following the same exact reasoning for crustal seismicity and rheology, the second, deeper peak in the strength profile (Fig. 1) is associated with seismic to aseismic transition in the uppermost lithospheric mantle.

It is not easy to estimate temperatures deep within the continental lithosphere. Nevertheless, using a global database, Chen and Molnar (1983) showed that the maximum depth of earthquakes in the continental crust also increases with tectonic age (or decreasing temperature), with a limiting temperature for crustal earthquakes of roughly 350 ± 100 °C. Notice that this value is close to the earlier estimate of Brace and Byerlee (1970). Recently, Behr and Platt (2011) used a combination of piezometry, thermobarometry and 2-D thermal modeling to study the history of deformation along the Whipple Mountains metamorphic core complex in southwestern US. They estimated that the transition of brittle to plastic deformation in the crust also occurred at a temperature of about 300 °C, further supporting the earlier estimates of limiting temperature for crustal earthquakes. Unfortunately, recent reports of limiting temperatures did not give uncertainties (Scholz, 1998; Boettcher et al., 2007). We suspect that such uncertainties are probably less than early estimates of Chen and Molnar (1983) but still in the order of ±50 to 100 °C.

In any case, a limiting temperature for seismicity indicates that the occurrence of earthquakes (a brittle process of frictional instability) diminishes at high temperatures when ductile mechanisms become dominant. Since the limiting temperature for mantle earthquakes is much higher than that for crustal seismicity (~650 °C vs. ~350 °C), in places where the geotherm places the uppermost mantle below ~650 °C and there is sufficient loading, mantle earthquakes are expected to occur. This reasoning completes the connection between a bimodal distribution of focal depths and the two peaks in the strength profile (Fig. 1).

Finally, in a series of studies to gain a holistic understanding of how continental rifts evolve, Buck (1991), Hopper and Buck (1996), and Keranen et al. (2009) showed with numerical simulations that the style of rifting seems to be tied to rheology of the continental lithosphere which, in turn, is mainly controlled by thermal state. When the geotherm is very high, neither the lower crust nor the uppermost mantle contributes much to the overall strength of a weak lithosphere. In effect the bottom of the lithosphere is at the level of the mid-crust and the style of extension is dominated by the formation of low-angle detachments (leading to metamorphic core-complexes) in the shallow crust. As a hot lithosphere cools, strength of the uppermost mantle becomes increasingly more important in determining the strength of the whole lithosphere, leading to wide rifts, such as the Basin and Range province of the western United States, and then eventually to narrow rift systems such as the currently active East African rift system. In other words, this model of rift evolution starts out with a modified "crème brûlée"rheology (as the lower crust is never strong) for a very hot lithosphere; as soon as the lithosphere begins cooling, it evolves into the "jelly sandwich" rheology for most of its life-cycle.

4.2. Bimodal distribution of focal depths

Depths of intra-continental earthquakes provide direct, *in situ*, observations of mechanical instability in the subsurface that complement numerical modeling and laboratory studies of rock physics. Moreover, the time-scale of the earthquake cycle is typically on the

order of 100 years, a value between that of geologic (millions of years) and laboratory (days to months) time-scales. In order to relate the distribution of focal depths to rheology of the lithosphere, it is important to address this issue in a sequence of three specific steps.

The very first step is to establish cases where the distribution of focal depths is bimodal. To this end, Chen and Yang (2004) and Yang and Chen (2008, 2010) presented both a significant amount of new data and detailed compilations for intra-continental regions in Asia and rifts in Africa, respectively. In the former case, eleven earthquakes, with magnitudes ranging from 4.9 to 6, occurred near and below the Moho beneath the western Himalayan syntaxis, the western Kunlun Mountains, and southern Tibet (near Xigaze) between 1963 and 1999. To date, there is no dispute regarding the reliability of precisely determined focal depths in any of these regions, and the distribution of focal depths is clearly bimodal in these regions where the subduction of oceanic lithosphere ceased tens of millions years ago.

Fig. 4 shows the tectonic context of an intriguingly deep event that occurred on October 25, 1990 at a depth of 100 ± 8 km below the western Himalayan syntaxis (event *H8* of Chen and Yang (2004)). This large (magnitude ~6) event occurred under the Lesser Himalayan terrane where the average elevation is only about 2 km, so the crust is unlikely to be 90 to100 km thick in this region (or anywhere else). The key point of Fig. 4 is to view this event in the context of the dense zone of earthquakes associated with remnant subduction zone(s) near the Hindu Kush. The Hindu Kush seismic zone (HKSZ) has a clear east–west trend, with a concentration of seismicity between depths of 150 and 250 km. Event *H8* is an isolated large earthquake that occurred some 150 km southward from the center of seismicity in the HKSZ (near 36.3°N, 71.0°E), and there is no straightforward geometry or any other supporting evidence to link this event to the HKSZ (Fig. 4).

In the case of recent studies by Yang and Chen (2008, 2010) in and around the entire East African rift system (EARS), both the comprehensiveness of dataset and the continent-scale of spatial coverage provide new insights for regions of active extension where most seismicity is associated with well-defined rifts whose lengths range from about 100 to 1000 km. Under well-developed but amagmatic rift segments, focal depths show a bimodal distribution, with peaks centered near depths of about 15 ± 5 km and 35 ± 5 km. This type of distribution occurs both along the main axis of the western branch of the EARS, including (from south to north) Lake Malawi, Lakes Tanganyika-Rukwa, and Lake Albert, as well as on short, individual rift segments of the northern Tanzania divergence (NTD) near the southern terminus of the Kenya rift, and those scattered in the western outboard region farther west of the western branch (Yang and Chen, 2010 and references therein).

In Fig. 5, we base the histograms on seismic moment, which not only is physically clear and geologically relevant, but also directly relates to elastic strain released by earthquakes (Kostrov, 1974; Chen and Molnar, 1977). If instead of seismic moment, one uses the number of earthquakes (e.g. Foster and Jackson, 1998; Albaric et al., 2009), a practice that exponentially emphasizes small earthquakes whose seismic moments are orders of magnitude less than those of large to moderate-sized events, bimodal distribution of seismicity remains. There are some subtle shifts between the two renditions, with differences in the depth of peaks that are comparable to the size of bins (5 km) (Yang and Chen, 2010 and references therein).

In essence, the bimodal distribution of focal depths shown in Fig. 5 is very similar to that of intra-continental earthquakes elsewhere, particularly in zones of recent convergence where the crust has thickened (e.g., Chen and Molnar, 1983; Chen and Kao, 1996; Zhu and Helmberger, 1996). In the case of Fig. 5, depth separating the two peaks in seismicity is naturally small in zones of active rifting where the crust most likely has been or is being thinned. This difference is superficial in that the two peaks of seismicity are always restricted to the upper/middle crust, and near the Moho and below, respectively.

The next question is whether the second peak of seismicity takes place entirely in the uppermost mantle or in the lower crust (Maggi et al., 2000; Jackson, 2002). The issue arises because precise knowledge of crustal thickness is usually unavailable near the source zone of unusually deep earthquakes, some of which occurred at depths close to rough estimates of where the Moho lies. However, there is ample evidence for cases of a gradual transition between the crust and the uppermost mantle in general (e.g., Eaton, 2006), rendering the issue somewhat moot.

While the quest of seeking precise position of the Moho near the second peak of seismicity continues, Yang and Chen (2010) showed direct evidence for sub-crustal earthquakes by determining the relative depth of mantle earthquakes below the Moho. This approach uses a first principle in seismology—measuring the difference in travel-times between the direct arrival and underside reflection off the Moho—to obtain the depth of mantle earthquakes relative to the Moho. These results are robust in that a number of observed *P*-wave trains, including both high-quality, individual seismograms at different azimuths and distances, and enhanced waveforms resulting from stacking by singular value decomposition, are precisely matched by synthetic seismograms, leaving little doubt in proving the existence of mantle earthquakes some 10 to 12 km below the crust, regardless of the actual position of the Moho (Yang and Chen, 2010). While the number of such earthquakes is small so far, their existence requires that the sub-continental mantle lithosphere in their source region is below about 600–700 °C and strong enough to sustain elastic stress over decadal to centenary time-scales. This conclusion does not rule out the possibility of some seismicity in the lowermost crust, especially in regions where the Moho is gradational (e.g., Chen and Molnar, 1983).

Third and finally, the question is whether the lower crust is weak in regions where the distribution of seismicity is bimodal. When this issue first came to the fore, most of the data are from the Tibetan plateau where seismicity concentrates in the upper crust and the uppermost mantle, but the level of seismicity in the greatly thickened crust is negligible between about 15 and 70 km (Chen et al., 1981; Chen and Yang, 2004; Monsalve et al., 2006). So a weak lower crust is inferred indirectly, as one cannot rule out pathological cases such as a near-rigid lower crust with negligible deformation but high levels of shear stress.

Along the EARS, Fig. 5 indicates that the minimum in seismicity between two peaks is low but not absent. Even so, it still favors the notion that there is a zone in the lower crust where stress must be lower than its neighboring regions above and below. The reason is twofold. First, earthquakes detectable at teleseismic distances prove that the lower crust is deforming, ruling out the pathologic case of a near-rigid zone between peaks of seismicity. Second, partial release of shear stress by plastic flow in the lower crust provides a straightforward interpretation for why a minimum in seismicity occurs in a number of different regions that are hundreds of kilometers apart along the EARS. Otherwise, there should be no clear pattern at all in the distribution of focal depths. This interpretation implies that under these segments of the EARS, the lower crust is in a region of brittle–ductile transition where plastic deformation dominates. Following this reasoning, the deep peak of seismicity, which includes the uppermost mantle and perhaps also the lowermost crust, is also in a state of brittle–ductile transition, but the level of shear stress is higher than that in the lower crust above and brittle deformation plays a significant role.

5. Field observations and simulations in the laboratory

Homburg et al. (2010) investigated rheological contrast between the lower crust and the uppermost mantle by carefully studying a mantle section of the Oman ophiolite where gabbronorite dikes intruded into host harzburgite (depleted oceanic mantle). The most salient observation is that subsequent deformation concentrated in the gabbronorite dikes, without apparent deformation in either the

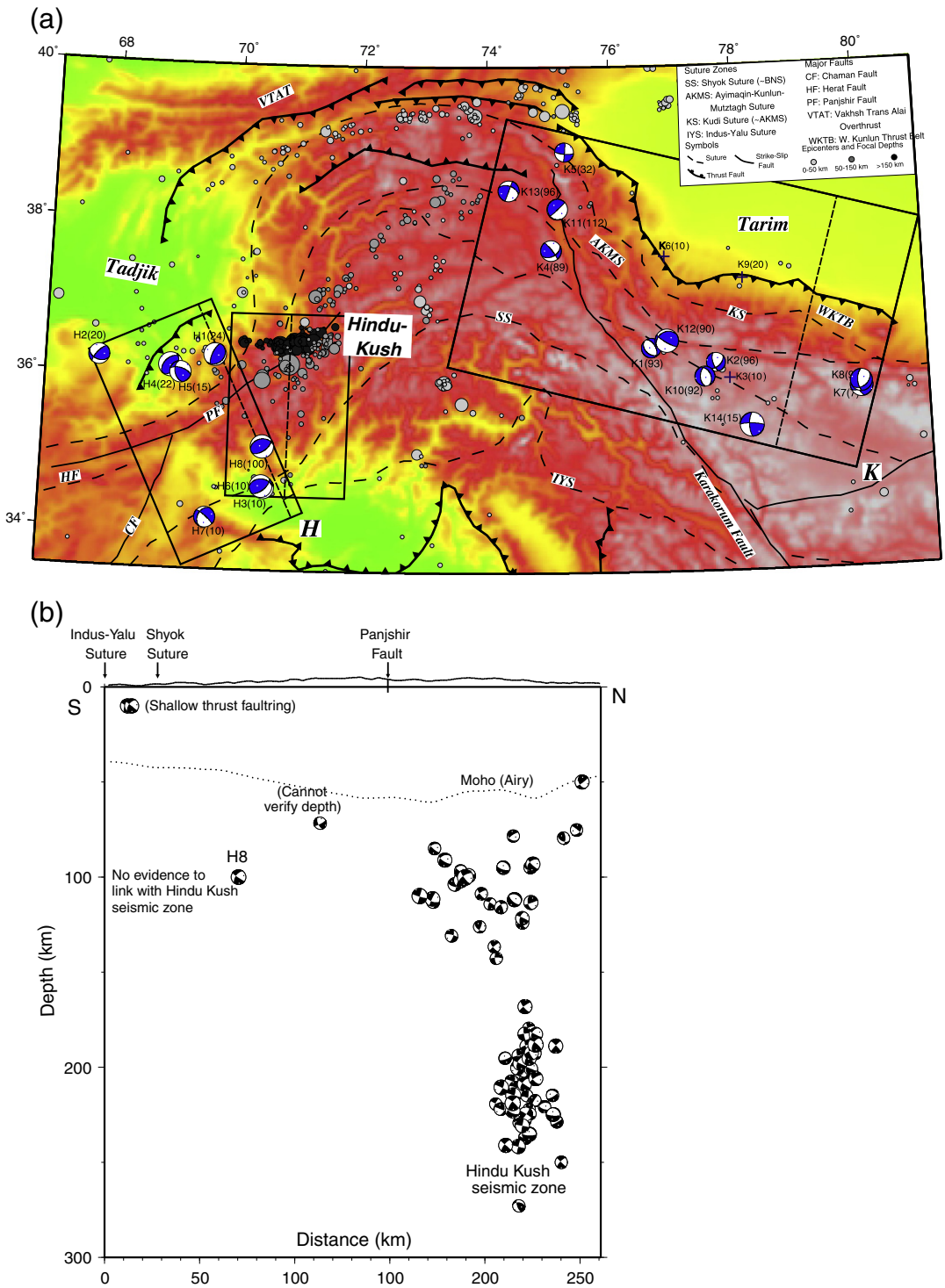

Fig. 4. (a) A map of the westernmost portion of the Himalayas and Tibet, showing epicenters and main geologic structures. Boxes enclose areas where mantle earthquakes occur: western Himalayan syntaxis (*H*), western Kunlun Mountains (*K*), and Hindu Kush. Dashed line in each box marks where cross-section is shown in (b) and Chen and Yang (2004). (Regions *H* and *K* are marked for easy comparison with earlier work only.) Key events are numbered as in Chen and Yang (2004), with precisely determined focal depths (in km) shown in parentheses. Focal mechanisms of earthquakes (large symbols) are represented by equal-area projections of the lower and the western focal sphere in maps and cross-sections, respectively. Shaded quadrants represent compression first motions of *P*-waves, while solid and open circles show *P*- and *T*-axes (or axes of maximum and minimum contractions), respectively. Crosses mark precise hypocenters without fault plane solutions. (b) North–south cross-section of the Hindu Kush region in (a), contrasting the east–west trending, intense seismicity down to depths of at least 250 km beneath the Hindu Kush with the isolated, large event *H8*.

pyroxenite or the host harzburgite. Homburg et al. (2010) concluded that plagioclase-rich lithology typical of the lower crust is at least two orders of magnitude less viscose than olivine-dominated harzburgite from the mantle.

The contrast in viscosity is an order of magnitude higher, if large strain associated with medial mylonites in gabbronorite dikes is used to estimate viscosity. This upper bound in viscosity contrast may be an overestimate as there is positive feedback between strain concentration and reduction in grain size of the mylonites. Nevertheless, concentration of stain in gabbronorite dikes is obvious even in regions where the grain sizes of both the gabbronorite and the harzburgite are comparable (Fig. 1b of Homburg et al. (2010)). It is worth noting that this work is the

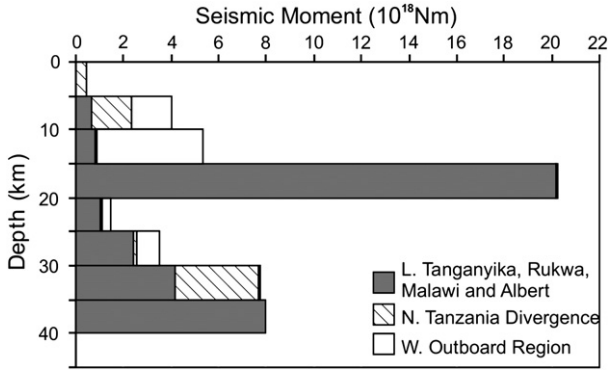

Fig. 5. A histogram summarizing bimodal distributions of seismic moment release as a function of depth along well-defined but amagmatic rift segments of the East African Rift system (from Yang and Chen(2010)). The data include all large- to moderate-sized earthquakes (m_b>4.6) between 1976 and early 2008. The bin-size used (5 km) is commensurate with uncertainties in focal depths (about ±3 km). A corresponding histogram plotted in logarithmic scale is shown in Fig. A5 of Yang (2009).

Fig. 6. Photographs of outcrops in the Western Gneiss Region of the Norwegian Calidonides showing lithological control on mode of deformation. In both cases, the predominant tectonic fabric is orogeny-parallel, formed during the latest stage of the orogen. Dark colored rocks are eclogite boudins formed with significant brittle component of deformation. Light colored country rocks are felsic gneiss that readily flowed. (a) Notice the sub-horizontal lineation and the fractured end of the large boudin. For scale, the top of the passing vehicle (foreground) is about 4 m in length and the cliff-face is about 30 m in height. (b) The standing person is about 1.8 m in height.

only study in which naturally exposed rocks, characteristic of the mantle and the lower crust, are examined together. In contrast, various discussions of pseudotachylytes and their implications for lithospheric strength dealt with either crustal or mantle materials in isolation (see discussions below), lacking the necessary context as in Homburg et al. (2010).

Preliminary results by Wang et al. (2009) also indicate that debate regarding the relative strength of the lower crust and the uppermost mantle may be on the verge of being resolved by laboratory experiments. The gist of the debate hinges on the role of volatiles in promoting plastic deformation: Could a dry, mafic lower crust be stronger than a wet, ultramafic mantle (Hirth and Kohlstedt, 1996; Mackwell et al., 1998)? Previously, there was no reliable measurement for mafic granulites, an under-saturated facies that was proposed as the best candidate for a strong lower continental crust (Maggi et al., 2000; Jackson, 2002). The preliminary report of Wang et al. (2009) showed that under laboratory conditions, dry, mafic granulite seems to be significantly weaker than wet peridotite (cf. Mackwell et al. (1998)). If this new result holds, it would be strong evidence for the lower crust being weaker than the uppermost mantle. Regardless of this issue, it is important to note that geological processes that could juxtapose dry, mafic granulite over wet peridotite remain to be identified.

The notion of a weak lower crust does not rule out a minor component of brittle deformation. In fact the distribution of focal depths (Fig. 5) and field observations of exhumed lower crust both support the interpretation that the lower crust is at the state of brittle–ductile transition (or more precisely the transition between stick-slip and stable sliding, but the difference between the two conditions is minor and it is difficult to distinguish in seismic and geodetic observations; see Chen and Kao (1996) for detailed discussions). A minor component of brittle deformation, however, offers no direct evidence for the interpretation that the lower crust is stronger than the uppermost mantle. To the contrary, many examples of brittle deformation in the field demonstrate the importance of lithological control over rheology.

Fig. 6 shows two examples from the Western Gneiss Region of the Norwegian Caledonides. In both cases, during the very last phase of Caledonian orogeny, numerous mafic dykes, metamorphosed into eclogite, were stretched and broken into large, discrete boudins. While the mafic boudins were apparently formed through brittle deformation, the surrounding crustal material of less mafic gneiss simply flows. In the language of classic geology, mafic rocks are more "competent" than less mafic varieties and Fig. 6 simply shows examples whose lengths approach the order of 100 m and were deformed under high pressures corresponding to the lower portion of a greatly thickened continental crust.

It is worth noting that the occurrence of pseudotachylytes—often taken to be the result of frictional melting during sudden slip of faults—among ductile shear zones in the Western Gneiss region of Norway was used as a direct argument for seismicity in a strong lower crust (e.g., Austrheim and Boundy, 1994; Jackson et al., 2004). This argument becomes highly problematic when one includes the occurrence of pseudotachylytes in exposed mantle peridotite, such as those reported by Anderson and Austrheim (2006) in Corsica and by Ueda et al. (2008) in the Alps. In the former case, the maximal length of pseudotachylytes in the mantle approaches 100 m, two to three orders of magnitude greater than that observed in the crust. So if the occurrence of pseudotachylytes indicates rheologically strong material, peridotite must be as strong as mafic granulite. Furthermore, longer pseudotachylytes would indicate greater earthquakes in the mantle than in the lower crust. Finally, the occurrence of pseudotachylytes does not necessarily indicate a dry lower crust either, as pseudotachylytes have been well documented long ago to occur in amphibolite facies where hydrous minerals such as biotite are abundant (e.g., Lundgren and Ebblin, 1972; Goldberg, 1992). Overall, we see no clear link between pseudotachylytes and strength profiles.

6. Discussions

6.1. Deep aftershocks

In light of tremors and low-frequency earthquakes—unconventional mode of strain release near the Moho—that occur 10–15 km below the zone of shallow crustal earthquakes (see Section 2), it is worth noting another pattern of focal depths in Africa: Yang and Chen (2008, 2010) noted that beyond both termini of well-defined portion of the western branch of the EARS, late aftershocks occur at depths 10–20 km below large (magnitude ~7) earthquakes in the top 15 km of the crust. In both cases, conventional indicators of active rifting, such as geomorphic expressions of normal faults or basins, are absent; yet active extension is evident from normal faulting focal mechanism associated with large earthquakes.

The earthquake sequence in May–July of 1990 occurred more than 300 km farther north of Lake Albert or the northern end of clear-defined western branch. A mixture of normal and strike-slip faulting is associated with the two largest shocks in the sequence (*Mw* ~7.1, Gaulon et al., 1992). Even though remnants of rifts of Mesozoic age and east–west trending striking strike-slip faults are buried beneath this area (Bosworth, 1992; Ebinger and Ibrahim, 1994; Ibrahim et al., 1996), there are no historical earthquakes to suggest that this isolated patch of seismicity is directly connected to the rest of the EARS. In this case, a moderate-sized event (W6 of Yang and Chen (2010), *Mw* ~4.8) occurred at a remarkable depth of 35 ± 3 km.

As recent as February of 2006, a comparable-sized earthquake sequence (main shock *Mw* ~7.0) occurred in Mozambique, showing a similar pattern of focal depths in an equivalent tectonic setting to that of the 1990 sequence more than 2500 km farther north. Focal mechanisms associated with the 2006 Mozambique sequence provide convincing evidence for active extension trending east–west, but the nearest, apparent geomorphic and structural expressions of rifting are at the southern tip of Lake Malawi, some 800 km north of the epicentral zone (Yang and Chen, 2008). The main shock and most aftershocks of the Mozambique sequence released a large amount of seismic moment at depths near 15 km, but one of the large aftershocks occurred at a considerably larger depth of 27 ± 3 km (W55of Yang and Chen (2010), *Mw* ~5.3).

While precise position of the Moho is not known in either case, the occurrence of conventional aftershocks below the shallow seismogenic zone resembles the configuration of tremors/low-frequency earthquakes near Parkfield and Tottori (Fig. 2). In the case of Parkfield, seismicity has been well monitored so it is unlikely that conventional earthquakes also occurred at depth but escaped detection. In Africa, seismic monitoring is sparse at best and it is unknown if tremors/low-frequency earthquakes exist. The cause of deep aftershocks is not well understood at the moment and Yang and Chen (2010) proposed that it is perhaps a response to high strain rate due to rapid loading of co-seismic slip, as proposed for aftershocks of the 1992 Landers earthquake in California (*M* ~7.3) (Rolandone et al., 2004). Intriguingly, migration of deep tremors along the San Andreas fault zone near Parkfield and period-doubling of their recurrence intervals also seem to have been influenced in some way by ruptures of significant earthquakes in the shallow seismogenic zone (Shelly, 2010a, 2010b). Whether deep aftershocks are somehow linked with tremors/low-frequency earthquakes awaits further investigation.

6.2. Stable terranes of SCML

Globally, other studies have defined stable terranes of SCML using a wide variety of criteria, including distribution of epicenters, seismic anomalies identified through travel-time tomography, patterns in isotopic ratios, and locations of near-surface geologic boundaries (e.g., Griffin et al., 2009 and references therein). Typically stable terranes have been defined rather liberally, often based on a single criterion. In our case, using a combination of complementing geophysical means (Chen et al., 2010; Hung et al., 2010; Nowack et al., 2010), we specifically identified only three blocks of SCML that remain stable through ongoing continental collision: those beneath the southern Lhasa and the northern Qiangtang terranes, and the Greater India.

Apparently, continental collision reassembles cratonic blocks but did not destroy them. Currently on the surface, the Himalayan collisional front is over 1000 km farther south of the southern edge of the Taidam basin—the closest stable terrane north of Tibet. Along the corridor near 84°E, where high resolution seismic data are readily available in the public domain (Chen et al., 2010), extrapolation of current rate of ground motion determined by GPS (Zhang et al., 2004; Chen and Tseng, 2007) predicts that the leading edge of Greater India will impinge upon the Tarim basin in about 15 Ma. By then, cratonic SCLM of Greater India would have remained distinct, stable for about 70 Ma since the onset of the collision.

In the case of the EARS, rifting does not seem to have readily divided cratonic SCML either. For instance, southward propagation of the Kenya rift, the southernmost rift unit of the eastern branch of the EARS, has been stalled at the northern Tanzania divergence (NTD), not penetrating deep into the interior of the Tanzania craton (e.g., Ebinger et al., 1997; Foster et al., 1997; Albaric et al., 2010). A number of reports have attributed characteristics of the NTD, including diffuse nature of faulting, scattered seismicity, and lateral (east–west) spread of recent volcanism as manifestations of how an active rift terminates on the periphery of a stable craton (e.g. Scholz et al., 1976; Fairhead and Henderson, 1977; Fairhead and Stuart, 1982; Nyblade and Langston, 1995; Foster and Jackson, 1998; Nyblade and Brazier, 2002). As Yang and Chen (2010) have noted, the southernmost volcanic rocks in the NTD initiated about 8 Ma ago (Dawson, 1992), indicating that southern tip of the Kenya rift has impinged upon the northern Tanzania craton since that time, but made little progress propagating farther southward.

This interpretation is consistent with the prediction of numerical modeling by Van Wijk and Blackman (2005): as a propagating rift encounters a mechanically strong terrane, high resistance to shear deformation effectively stalls rift propagation, limiting deformation to the periphery of a craton. In addition, the same study predicted the buildup of shear stress near the tip of the stalled rift tends to cause spatially distributed extension. At any rate, as the occurrence of unusually deep earthquakes under the NTD reflects great shear strength of an old, cold craton where elastic strain can build up to be released by brittle slip at considerable depth (Chen and Molnar, 1983; Yang and Chen, 2010), rifting does not easily destabilize a craton.

6.3. Epilogue

While we, as well as many others, have emphasized lithological control over the contrast in viscosity across the Moho, it is important to reemphasize that both experimental and theoretical considerations point to the key importance of temperature in limiting ductile strength (e.g., Homburg et al., 2010). In other words, lithological control largely reflects the difference in limiting temperatures between ultramafic mantle and less mafic crust. Chen and Molnar (1983) followed this reasoning closely and provided estimates of limiting temperatures of about 700 ± 100 °C and 350 ± 100 °C for the mantle and the crust, respectively. Based on more recent results of experimental rock mechanics and thermal models of the oceanic lithosphere, the limiting temperatures are slightly lower, about 650 °C and 350 °C (with uncertainties of approximately ±50 to 100 °C for both cases).

Using the latter value as a starting point, for a nominal crustal thickness of 35 km, the entire crust will be seismogenic, if the geotherm is close to 10 K/km (see Chen and Molnar (1983) for specific regions where this may be the case.) As such, the entire crust is strong enough to accumulate elastic stress but the uppermost mantle would also be

strong; so one could view this scenario as a variant of the "crème brûlée" model but the strong layer is thick, comprised of the entire crust as well as the uppermost mantle. If the geotherm is close to 15 K/km, then only the top two-thirds of the crust is expected to be seismogenic, resulting in a "jelly sandwich" rheology. (At even higher geotherms, such as the extensional setting for forming low-angle detachments, the uppermost mantle would be too hot to sustain earthquakes and lithospheric strength, which is small overall, would largely reside in the upper/middle crust (Buck, 1991; Hopper and Buck, 1996; Keranen et al., 2009).

Now suppose the crust has doubled its thickness but sufficient time has elapsed for the geotherm to recover to about 15 °C/km, then only the top one-third of the crust would be seismogenic. This simple exercise provides a straightforward explanation for why bimodal distribution of focal depths is most pronounced in places such as Tibet. While there does not appear to be a good estimate of the geotherm available under Tibet, Chen and Molnar (1981) estimated that the temperature in the uppermost mantle of southern Tibet is about 250 °C greater than that under cratons, or between 650 °C and just below 800 °C, with the range largely reflecting uncertainties in determining temperatures under cratons. At any rate, these rough estimates of temperature in the uppermost mantle are low enough to be compatible with a limiting temperature of about 600–700 °C for mantle earthquakes (Chen and Molnar, 1983; Wiens and Stein, 1983; McKenzie et al., 2005).

While bimodal distributions of focal depths indicate a minimum in strength between the two peaks of seismicity, such a minimum does not automatically imply negligible coupling between the upper crust and the lithospheric mantle. Recall that effective viscosity is the ratio between shear stress and strain rate. Even when effective viscosity is low, the stress can be high under high strain rate that can easily arise across a very thin channel of shear.

Another caveat is that when using seismicity data, it is important to bear in mind that all earthquakes are not created equal. The seismic moment of a significant earthquake, such as the mantle event *H8* under the Lesser Himalayas (M_W ~6, Fig. 4), is about 24 million times that of a micro-earthquake of magnitude 1. Equally important is to make the distinction between micro-seismicity related to magma migration/intrusion and large earthquakes that reflect shearing instability during tectonic faulting. The two types of seismicity result from fundamentally different causes and are readily distinguishable from each other (Wolfe et al., 2003). This is particularly critical near magma-rich rifts and other regions of active volcanism. For instance, along the Ethiopian rift, dikes appear to intrude into the upper crust (Bendick et al., 2006) and may have caused micro-seismicity associated with igneous intrusion (Keir et al., 2006). A recent study reported that this type of micro-seismicity seems common in the lower crust under the Ethiopian rift (Keir et al., 2009), but these activities have little bearing on the current discussion, just as volcanic tremors are irrelevant to low-frequency earthquakes.

7. Concluding remarks

Results based on high resolution, dense-spaced seismic data from Project Hi-CLIMB indicate that stable, therefore strong, lithospheric mantle—marked by flay-lying, laterally continuous Moho—persists through repeated continental collision under both the Lhasa and Qiangtang terranes of Tibet (Nowack et al., 2010). Centered around a depth of 200 km, a slab-like, regional feature of high V_P and V_S extends from the Himalaya collision front beyond the BNS, near the latitude of 33°N in places (Chen and Özalaybey, 1998; Chen et al., 2010; Hung et al., 2010, 2011). This feature is interpreted as underthrust Greater Indian shield that has advanced sub-horizontally northward by some 600 km beyond the collisional front and we attribute the longevity of Greater India to compositional buoyancy and high strength of depleted Archean SCLM (e.g., Jordan, 1978, 1988).

There is little doubt that bimodal distribution of earthquake focal depths, with peaks in the upper/middle crust and near the Moho, dominates in certain regions (Chen and Yang, 2004; Yang and Chen, 2010). This pattern is a longstanding proxy for similar distribution in strength of the continental lithosphere ("jelly sandwich" rheology). There is now strong evidence that large earthquakes occur below the mantle (Chen and Yang, 2004; Yang and Chen, 2010), even though the second peak of seismicity may not be entirely in the upper mantle, especially in places where the crust–mantle transition is gradual. Intriguingly, non-volcanic tremors/low-frequency earthquakes also occur near the Moho, notably along the Parkfied region of the San Andreas fault system and in southwestern Japan. These new-found modes of strain release take place below the seismogenic zone in the shallow crust, leaving a gap of 10 km or more of the lower crust completely devoid of any seismic radiation.

Sizable uncertainties notwithstanding, limiting temperatures for seismogenesis provide a simple rule and a valuable concept for understanding the distribution of focal depths. Under laboratory conditions, the limiting temperature marks the termination of frictional instability which, in turn, is close to the onset of crystal plasticity. As such, lithological effect in rheology is reflected by the difference in limiting temperatures between mantle and crustal materials (Chen and Molnar, 1983).

In terms of field observations, pseudotachylites occur in both peridotites and mafic granulites (Austrheim and Boundy, 1994; Anderson and Austrheim, 2006, respectively), thus providing no direct information regarding the strength of host materials. In the crust, pseudotachylites occur in rocks of granulite facies and those of amphibolite facies with abundant hydrous minerals (e.g., Lundgren and Ebblin, 1972; Goldberg, 1992), therefore not an indicator of water content of host rocks either. In the case where both mantle and lower crustal mineral assemblages are exposed, *in situ*, next to each other, the viscosity of lower crustal material is two orders of magnitude less than that of the mantle (Homburg et al., 2010).

Acknowledgements

The late C. Goetze assigned the extrapolation of flow laws determined from laboratory experiments as a homework problem in his graduate-level class in the mid-1970s, marking Chen's first exposure to rheology of the continental lithosphere. Since then, many colleagues encouraged him to continue this line of research and several programs of the U.S. National Science Foundation, including Geophysics, Continental Dynamics, and Cooperative Studies of the Earth's Deep Interior, provided continual support that allowed the senior author to pursue studies related to the current subject whenever an impetus arose. In addition, P. Robinson, D. Gee, and their colleagues showed Chen key outcrops in the Scandinavian Calidonides. An anonymous reviewer provided helpful comments on experimental rock mechanics and the Editor-in-Chief, M. Santosh, also made suggestions to improve the manuscript. Chen also benefited from discussions with R. Bendick, G. Hirth, C.T. Lee, and D. Shelly. Direct financial support for this study came from NSF grants EAR99-09362 ("Hi-CLIMB"), EAR05-51995, EAR06-35419, EAR06-35611 (R.L.N.) and US Air Force/Department of Energy contract FA8718-08-C-002. Any opinions, findings and conclusions or recommendations expressed in this material are those of the authors and do not necessarily reflect those of the NSF.

References

Aki, K., Richards, P.G., 2002. Quantitative Seismology. Univ. Sci. Books, Sausalito, CA. 704 pp.

Albaric, J., Déverchère, J., Petit, C., Perrot, J., LeGall, B., 2009. Crustal rheology and depth distribution of earthquakes: insights from the central and southern East African Rift System. Tectonophysics 468, 28–41. doi:10.1016/j.tecto.2008.05021.

Albaric, J., Perrot, J., Déverchère, J., Deschamps, A., Gall, B.L., Ferdinand, R.W., Petit, C., Tiberi, C., Sue, C., Songo, M., 2010. Contrasted seismogenic and rheological

behaviours from shallow and deep earthquake sequences in the North Tanzanian Divergence, East Africa. Journal of African Earth Sciences 58, 799–811.
Anderson, T.B., Austrheim, H., 2006. Fossil earthquakes recorded by pseudotachylytes in mantle peridotite from the Alpine subduction complex of Corsica. Earth and Planetary Science Letters 242, 58–72.
Artemieva, I., Thybo, H., 2008. Deep Norden: highlights of the lithospheric structure of Northern Europe, Iceland, and Greenland. Episodes 33, 98–106.
Austrheim, H., Boundy, T.M., 1994. Pseudotachylytes generated during seismic faulting and eclogitization of the deep crust. Nature 265, 82–83.
Bakun, W.H., Aagaard, B., Dost, B., Ellsworth, W.L., Hardebeck, J.L., Harris, R.A., Ji, C., Johnston, M.J.S., Langbein, J., Lienkaemper, J.J., Michael, A.J., Murray, J.R., Nadeau, R.M., Reasenberg, P.A., Reichle, M.S., Roeloffs, E.A., Shakal, A., Simpson, R.W., Waldhauser, F., 2005. Implications for prediction and hazard assessment from the 2004 Parkfield earthquake. Nature 437, 969–974.
Beghoul, N., Barazangi, M., Isacks, B., 1993. Lithospheric structure of Tibet and western North America: mechanisms of uplift and a comparative study. Journal of Geophysical Research 98, 1997–2016.
Behr, W.M., Platt, J.P., 2011. A naturally constrained stress profile through the middle crust in an extensional terrane. Earth and Planetary Science Letters 303, 181–192.
Bendick, R., McClusky, S., Bilham, R., Asfaw, L., Klemperer, S., 2006. Distributed Nubia–Somalia relative motion and dike intrusion in the Main Ethiopian Rift. Geophysical Journal International 165, 303–310.
Blanpied, M.L., Lockner, D.A., Byerlee, J.D., 1991. Fault stability inferred from granite sliding experiments at hydrothermal conditions. Geophysical Research Letters 18, 609–612.
Bleibinhaus, F., Hole, J.A., Ryberg, T., Fuis, G.S., 2007. Structure of the California Coast Ranges and San Andreas Fault at SAFOD from seismic waveform inversion and reflection imaging. Journal of Geophysical Research 112, B06315. doi:10.1029/2006JB004611.
Boettcher, M.S., Hirth, G., Evans, B., 2007. Olivine friction at the base of oceanic seismogenic zones. Journal of Geophysical Research 112. doi:10.1029/2006JB004301.
Bostock, M.G., Rondenay, S., Shragge, J., 2001. Multiparameter two-dimensional inversion of scattered teleseismic body waves 1. Theory for oblique incidence. Journal of Geophysical Research 106, 30771–30782.
Bosworth, W., 1992. Mesozoic and early Tertiary rift tectonics in East Africa. Tectonophysics 209, 115–137.
Brace, W.F., Byerlee, J.D., 1970. California earthquakes: why only shallow focus? Science 168, 1573–1576.
Brueckner, H.K., Van Roermund, H.L.M., 2004. Dunk tectonics: a multiple subduction/eduction model for the evolution of the Scandianvian Caledonides. Tectonics 23. doi:10.1029/2003TC001502.
Buck, W.R., 1991. Modes of continental lithospheric extension. Journal of Geophysical Research 96, 20,161–20,178.
Burov, E., Watts, A.B., 2006. The long-term strength of continental lithosphere: "jelly sandwich" or "crème brûlée"? GSA Today 16. doi:10.1130/1052-5173.
Chen, W.-P., Kao, H., 1996. Seismotectonics of Asia: some recent progress. In: Yin, A., Harrison, M. (Eds.), The Tectonic Evolution of Asia. Cambridge Univ. Press, Palo Alto, pp. 37–62.
Chen, W.-P., Molnar, P., 1977. Seismic moments of major earthquakes and the average rate of slip in Asia. Journal of Geophysical Research 82, 2945–2969.
Chen, W.-P., Molnar, P., 1981. Constraints on seismic wave velocity structure beneath the Tibetan plateau and their tectonic implications. Journal of Geophysical Research 86, 5937–5962.
Chen, W.-P., Molnar, P., 1983. Focal depths of intracontinental and intraplate earthquakes and their implications for the thermal and mechanical properties of the lithosphere. Journal of Geophysical Research 88, 4183–4214.
Chen, W.-P., Özalaybey, S., 1998. Correlation between seismic anisotropy and Bouguer gravity anomalies in Tibet and its implications for lithospheric structures. Geophysical Journal International 135, 93–101.
Chen, W.-P., Tseng, T.-L., 2007. Small 660-km seismic discontinuity beneath Tibet implies resting ground for detached lithosphere. Journal of Geophysical Research 112, B05309. doi:10.1029/2006JB004607.
Chen, W.-P., Yang, Z.-H., 2004. Earthquakes beneath the Himalayas and Tibet: evidence for strong lithospheric mantle. Science 304, 1949–1952.
Chen, W.-P., Nábelek, J.L., Fitch, T.J., Molnar, P., 1981. An intermediate depth earthquake beneath Tibet: source characteristics of the event of September 14, 1976. Journal of Geophysical Research 86, 2863–2876.
Chen, Q., Freymueller, J.T., Wang, Q., Yang, Z., Xu, C., Liu, J., 2004. A deforming block model for the present-day tectonics of Tibet. Journal of Geophysical Research 109. doi:10.1029/2002JB002151.
Chen, W.-P., Martin, M., Tseng, T.-L., Nowack, R.L., Hung, S.-H., Huang, B.-S., 2010. Shear-wave birefringence and current configuration of converging lithosphere under Tibet. Earth and Planetary Science Letters 295, 297–304. doi:10.1016/j.epsl.2010.04.017.
Chung, S.-L., Chu, M.-F., Zhang, Y., Xie, Y., Lo, C.-H., Lee, T.-Y., Lan, C.-Y., Li, X., Zhang, Q., Wang, Y., 2005. Tibetan tectonic evolution inferred from spatial and temporal variations in post-collisional magmatism. Earth-Science Reviews 68, 173–196.
Dawson, J.B., 1992. Neogene tectonics and volcanicity in the North Tanzania sector of the Gregory Rift Valley: contrasts with the Kenya sector. Tectonophysics 204, 81–92.
Eaton, D.W., 2006. Multi-genetic origin of the continental Moho: insights from Lithoprobe. Terra Nova 18, 34–43.
Ebinger, C.J., Ibrahim, A.E., 1994. Multiple episodes of rifting in Central and East Africa: a re-evaluation of gravity data. Geologische Rundschau 83, 689–702.
Ebinger, C., Djomani, Y.P., Mbede, E., Foster, A.N., Dawson, J.B., 1997. Rifting Archaean lithosphere; the Eyasi–Manyara–Natron rifts, East Africa. Journal of the Geological Society of London 154, 947–960.
Evans, B., Kohlstedt, D.L., 1995. Rheology of rocks. Rock Physics and Phase Relations: A Handbook of Physical Constants. American Geophysical Union, Washington D.C., pp. 148–165.
Fairhead, J.D., Henderson, N.B., 1977. The seismicity of southern Africa and incipient rifting. Tectonophysics 41, T19–T26.
Fairhead, D., Stuart, G.W., 1982. The seismicity of the East African Rift System and comparison with other continental rifts. In: Palmason, G. (Ed.), Continental and Oceanic Rifts. American Geophysical Union, Washington, D.C., pp. 41–61.
Faul, U.H., Jackson, I., 2005. The seismological signature of temperature and grain size variations in the upper mantle. Earth and Planetary Science Letters 234, 119–134.
Foster, A.N., Jackson, J.A., 1998. Source parameters of large African earthquakes: implications for crustal rheology and regional kinematics. Geophysical Journal International 134, 422–448.
Foster, A.N., Ebinger, C., Mbede, E., Rex, D., 1997. Tectonic development of the northern Tanzanian sector of the East African Rift system. Journal of the Geological Society of London 154, 689–700.
Gaulon, R., Chorowicz, J., Vidal, G., Romanowicz, B., Roult, G., 1992. Regional geodynamic implications of the May–July 1990 earthquake sequence in southern Sudan. Tectonophysics 209, 87–103.
Goetze, C., 1978. The mechanism of creep in olivine. Philosophical Transactions of the Royal Society of London. Series A 288, 99–119.
Goldberg, D., 1992. Crosshole lithotectonic correlation in high-grade metamorphic rocks, central southern Connecticut. Geophysical Research Letters 19, 1879–1882.
Goleby, B.R., Shaw, R.D., Wright, C., Kennett, B.L., Lambert, K., 1998. Geophysical evidence for 'Thick-skinned' crustal deformation in central Australia. Nature 337, 325–330.
Griffin, W.L., O'Reilly, S.Y., Afonso, J.C., Begg, G.C., 2009. The composition and evolution of lithospheric mantle: a re-evaluation and its tectonic implications. Journal of Petrology 50, 1185–1204.
Hirth, G., Kohlstedt, D.L., 1996. Water in the oceanic upper mantle; implications for rheology, melt extraction and the evolution of the lithosphere. Earth and Planetary Science Letters 114, 93–108.
Hirth, G., Kohlstedt, D.L., 2003. Rheology of the upper mantle and the mantle wedge: a view from the experimentalists. Geophysics Monograph 138, 83–105.
Homburg, J.M., Hirth, G., Kelemen, P.B., 2010. Investigation of the strength contrast at the Moho: a case study from the Oman ophiolite. Geology 38, 679–682.
Hopper, J., Buck, W.R., 1996. The effect of lower crustal flow on continental extension and passive margin formation. Journal of Geophysical Research 101, 20,175–20,194.
Hung, S.-H., Chen, W.-P., Chiao, L.-Y., Tseng, T.-L., 2010. First multi-scale, finite-frequency tomography illuminates 3-D anatomy of the Tibetan Plateau. Geophysical Research Letters 37. doi:10.1029/2009GL041875.
Hung, S.-H., Chen, W.-P., Chiao, L.-Y., 2011. A data-adaptive, multi-scale approach of finite-frequency, travel-time tomography with special reference to P- and S-wave data from central Tibet. Journal of Geophysical Research 116, B06307. doi:10.1029/2010JB008190.
Ibrahim, A.E., Ebinger, C.J., Fairhead, J.D., 1996. Lithospheric extension northwest of the Central African Shear Zone in Sudan from potential field studies. Tectonophysics 255, 79–97.
Ide, S., Beroza, G.C., Shelly, D.R., Uchide, T., 2007. A scaling law for slow earthquakes. Nature 447, 76–79.
Jackson, J., 2002. Strength of the continental lithosphere: time to abandon the jelly sandwich? GSA Today (Sept. 2002), 4–10.
Jackson, J.A., Austrheim, H., McKenzie, D., Priestley, K., 2004. Metastability, mechanical strength, and the support of mountain belts. Geology 32, 625–628.
Jimenez-Munt, I., Fernandez, M., Verges, J., Platt, J.P., 2008. Lithosphere structure underneath the Tibetan plateau inferred from elevation, gravity and geoid anomalies. Earth and Planetary Science Letters 267, 276–289. doi:10.1016/j.epsl.20078.11.045.
Jin, Y., McNutt, M.K., Zhu, Y.-S., 1996. Mapping the descent of Indian and Eurasian plates beneath the Tibetan plateau from gravity anomalies. Journal of Geophysical Research 101, 11,275–11,290.
Jordan, T.H., 1978. Composition and development of the continental tectosphere. Nature 274, 544–548.
Jordan, T.H., 1988. Structure and formation of the continental tectosphere. Journal of Petrology Special Lithosphere Issue 11–37.
Karato, S.-I., 2010. Rheology of the Earth's mantle: a historical review. Gondwana Research 18, 17–45.
Karato, S., 2010. Rheology of the deep upper mantle and its implications for the preservation of the continental roots: a review. Tectonophysics 481, 82–98.
Keir, D., Ebinger, C., Stuart, G.W., Daly, E., Ayele, A., 2006. Strain accommodation by magmatism and faulting as rifting proceeds to breakup; seismicity of the northern Ethiopian Rift. Journal of Geophysical Research 111. doi:10.1029/2005JB003748.
Keir, D., Bastow, I.D., Whaler, K.A., Daly, E., Cornwell, D.G., Hautot, S., 2009. Lower crustal earthquakes near the Ethiopian rift induced by magmatic processes. Geochemistry Geophysics Geosystems 10. doi:10.1029/2009GC002382.
Keranen, K.M., Klemperer, S.L., Julia, J., Lawrence, J.F., Nyblade, A.A., 2009. Low lower crustal velocity across Ethiopia: is the Main Ethiopian Rift a narrow rift in a hot craton? Geochemistry Geophysics Geosystems 10, Q0AB01. doi:10.1029/2008GC002293.
Kostrov, V.V., 1974. Seismic moment and energy of earthquakes, and seismic flow of rock. Izvestiya, Academy of Sciences, USSR, Physics of the Solid Earth, English Translation 1, 23–44.
Lee, C.T.A., 2003. Compositional variation of density and seismic velocities in natural peridotites at STP conditions: implications for seismic imaging of compositional heterogeneities in the upper mantle. Journal of Geophysical Research 108, 2441. doi:10.1029/2003JB002413.

Lundgren, L., Ebblin, C., 1972. Honey Hill fault in eastern Connecticut: regional relations. Geological Society of America Bulletin 83, 2773–2794.
Mackwell, S.J., Zimmerman, M.E., Kohlstedt, D.L., 1998. High-temperature deformation of dry diabase with application to tectonics of Venus. Journal of Geophysical Research 103, 975–984.
Maggi, A., Jackson, J.A., McKenzie, D., Priestley, K., 2000. Earthquake focal depths, effective elastic thickness, and the strength of the continental lithosphere. Geology 28, 495–498.
Marillier, F., Keen, C.E., Stockmal, G., Quinlan, G., Williams, H., Colman-Sadd, S.P., O'Brien, S.J., 1989. Crustal structure and surface zonation of the Canadian Appalachians: implications of deep seismic reflection data. Canadian Journal of Earth Sciences 26, 305–321.
McBride, J.H., Brown, L.D., 1986. Reanalysis of the COCORP deep seismic reflection profile across the San Andreas Fault, Parkfield, California. Bulletin of the Seismological Society of America 76, 1668–1686.
McKenzie, D., Fairhead, D., 1997. Estimates of the effective elastic thickness of the continental lithosphere from Bouguer and free air gravity anomalies. Journal of Geophysical Research 102, 27,523–27,552.
McKenzie, D., Jackson, J., Priestley, K., 2005. Thermal structure of oceanic and continental lithosphere. Earth and Planetary Science Letters 233, 337–349.
Meade, B.J., 2007. Present-day kinematics at the India–Asia collision zone. Geology 35, 81–84.
Molnar, P., Chen, W.-P., 1984. *S–P* travel time residuals and lateral inhomogeneity in the mantle beneath Tibet and the Himalaya. Journal of Geophysical Research 89, 6911–6917.
Monsalve, G., Sheehan, A., Schuttle-Pelkum, V., Rajaure, S., Pandey, M.R., Wu, F., 2006. Seismicity and one-dimentional velocity structure of the Himalayan collision zone; earthquakes in the crust and upper mantle. Journal of Geophysical Research 111. doi:10.1029/2005JB004062.
Murray, J., Langbein, J., 2006. Slip on the San Andreas Fault at Parkfield, California, over two earthquake cycles, and the implications for seismic hazard. Bulletin of the Seismological Society of America 96, S283–S303. doi:10.1785/0120050820.
Nadeau, R.M., Dolenc, D., 2005. Nonvolcanic tremors deep beneath the San Andreas Fault. Science 307, 389. doi:10.1126/science.1107142.
Nadeau, R.M., Johnson, L.R., 1998. Seismological studies at Parkfield VI: moment release rates and estimates of source parameters for small repeating earthquakes. Bulletin of the Seismological Society of America 88, 790–814.
Nowack, R.L., Chen, W.-P., Tseng, T.-L., 2010. Application of Gaussian beam migration to multi-scale imaging of the lithosphere beneath the Hi-CLIMB array in Tibet. Bulletin of the Seismological Society of America 100, 1743–1754.
Nyblade, A.A., Brazier, R.A., 2002. Precambrian lithospheric controls on the development of the East African Rift system. Geology 30, 755–758.
Nyblade, A.A., Langston, C.A., 1995. East African earthquakes below 20 km depth and their implication for crustal structure. Geophysical Journal International 121, 49–62.
Ohmi, S., Hirose, I., Mori, J.J., 2004. Deep low-frequency earthquakes near the downward extension of the seismogenic fault of the 2000 Western Tottori earthquake. Earth Planets and Space 56, 1185–1189.
Owens, T.J., Zandt, G., 1997. Implications of crustal property variations for models of Tibetan plateau evolution. Nature 387, 37–43.
Ozacar, A.A., Zandt, G., 2009. Crustal structure and seismic anisotropy near the San Andreas Fault at Parkfield, California. Geophysical Journal International 178, 1098–1104.
Parsons, B., Sclater, J.G., 1977. An analysis of the variation of ocean floor bathymetry and heat flow with age. Journal of Geophysical Research 82, 803–827.
Poirier, J.-P., 1995. Plastic rheology of crystals. Mineral Physics and Crystallography: A Handbook of Physical Constants. American Geophysical Union, Washington, D.C., pp. 237–247.
Rolandone, F., Bürgmann, R., Nadeau, R.M., 2004. The evolution of the seismic–aseismic transition during the earthquake cycle: constraints from the time-dependent depth distribution of aftershocks. Geophysical Research Letters 31. doi:10.1029/2004GL021379.
Santosh, M., Maruyama, S., Yamamoto, S., 2009. The making and breaking of supercontinents: some speculations based on superplumes, super downwelling and the role of tectosphere. Gondwana Research 15, 324–341.
Savage, J.C., 1993. The Parkfield prediction fallacy. Bulletin of the Seismological Society of America 83, 1–6.
Scholz, C.H., 1990. Mechanics of Earthquakes and Faulting. Cambridge Univ. Press, Cambridge. 439 pp.
Scholz, C.H., 1998. Earthquakes and friction laws. Nature 391, 37–42.
Scholz, C.H., Koczynski, T.A., Hutchins, D.G., 1976. Evidence for incipient rifting in southern Africa. Geophysical Journal of the Royal Astronomical Society 44, 135–144.
Shapiro, S.S., Hager, B.H., Jordan, T.H., 1999a. Stability and dynamics of the continental tectosphere. Lithos 48, 115–133.
Shapiro, S.S., Hager, B.H., Jordan, T.H., 1999b. The continental tectosphere and Earth's long-wavelength gravity field. Lithos 48, 115–133.
Shelly, D.R., 2010a. Migrating tremors illuminate complex deformation beneath the seismogenic San Andreas Fault. Nature 463, 648–653. doi:10.1038/nature08755.
Shelly, D.R., 2010b. Periodic, chaotic, and doubled earthquake recurrence intervals on the deep San Andreas Fault. Science 328, 1385–1388. doi:10.1126/science.1189741.
Shelly, D.R., Hardebeck, J.L., 2010. Precise tremor source locations and amplitude variations along the lower-crustal central San Andreas Fault. Geophysical Research Letters 37. doi:10.1029/2010GL043672.
Sieh, K.E., 1978. Central California foreshocks of the great 1857 earthquake. Bulletin of the Seismological Society of America 68, 1731–1749.
Stesky, R., Brace, W.F., Riley, D.K., Robin, P.-Y.F., 1974. Friction in faulted rock at high temperature and pressure. Tectonophysics 23, 177–203.
Thatcher, W., 2007. Microplate model for the present-day deformation of Tibet. Journal of Geophysical Research 112. doi:10.1029/2005JB004244.
Tse, S.T., Rice, J.R., 1986. Crustal earthquake instability in relation to the depth variation of frictional slip properties. Journal of Geophysical Research 91, 9452–9472.
Tseng, T.-L., Chen, W.-P., Nowack, R.L., 2009. Northward thinning of Tibetan crust revealed by virtual seismic profiles. Geophysical Research Letters 36, L24304. doi:10.1029/2009GL040457.
Ueda, T., Obata, M., Di Toro, G., Kanagawa, K., Ozawa, K., 2008. Mantle earthquakes frozen in mylonitized ultramafic pseudotachylytes of spinel–lherzolite facies. Geology 36, 607–610.
Van Wijk, J.W., Blackman, D.K., 2005. Dynamics of continental rift propagation: the end-member modes. Earth and Planetary Science Letters 229, 247–258.
Vrijmoed, J.C., Smith, D.C., Van Roermund, H.L.M., 2008. Raman confirmation of micro-diamond in the Svartberget Fe–Ti type garnet-peridotite, Western Gneiss Region, Norway. Terra Nova 20, 295–301.
Wagner, L., Anderson, M., Jackson, J.M., Beck, S.L., Zandt, G., 2008. Seismic evidence for orthopyroxene enrichment in the continental lithosphere. Geology 36, 935–938.
Waldhauser, F., Schaff, D.P., 2008. Large-scale relocation of two decades of northern California seismicity using cross-correlation and double-difference methods. Journal of Geophysical Research 113. doi:10.1029/2007JB005479.
Walter, A.W., Mooney, W.D., 1982. Crustal structure of the Diablo and Gabilan ranges, central California: a reinterpretation of existing data. Bulletin of the Seismological Society of America 72, 1567–1590.
Wang, Y., Zhang, J., Green, H.W., Jin, Z., 2009. Petrofabrics and seismic properties of experimentally deformed granulites (abstract). EOS Transactions American Geophysical Union 90 FM_V54B-04.
Watts, A.B., Burov, E., 2003. Lithospheric strength and its relationship to the elastic and seismogenic layer thickness. Earth and Planetary Science Letters 213, 113–131.
Watts, A.B., Bodine, J.H., Steckler, M.S., 1980. Observations of flexure and the state of stress in the oceanic lithosphere. Journal of Geophysical Research 85, 6369–6376.
Wiens, D.A., Stein, S., 1983. Age dependence of oceanic intraplate seismicity and implications for lithospheric evolution. Journal of Geophysical Research 88, 6455–6468.
Wolfe, C.J., Okubo, P.G., Shearer, P.M., 2003. Mantle fault zone beneath Kilauea volcano, Hawaii. Science 300, 478–480.
Yang, Z.-H., 2009. Seismic studies of the East African Rift system and the Tibetan plateau: implications for the rheology of lithosphere and the evolution of rifts in continents, Ph.D thesis, University of Illinois, Urbana-Champaign.
Yang, Z.-H., Chen, W.-P., 2008. The Mozambique earthquake sequence of 2006: high-angle normal faulting in southern Africa. Journal of Geophysical Research 113, B12303. doi:10.1029/2007JB005419.
Yang, Z.-H., Chen, W.-P., 2010. Earthquakes along the East African Rift System: a system-wide, multi-scale perspective. Journal of Geophysical Research 115, B12309. doi:10.1029/2009JB006779.
Yin, A., Harrison, T.M., 2000. Geologic evolution of the Himalayan–Tibetan orogen. Annual Review of Earth and Planetary Sciences 28, 211–280.
Zhang, P.-Z., Shen, Z.-K., Wang, M., Gan, W., Burgmann, R., Molnar, P., Wang, Q., Niu, Z., Sun, J., Wu, J., Sun, H., You, X., 2004. Continuous deformation of the Tibetan Plateau from global positioning system data. Geology 32, 809–812.
Zhu, L., Helmberger, D.V., 1996. Intermediate depth earthquakes beneath the India–Tibet collision zone. Geophysical Research Letters 23, 435–438.

Wang-Ping Chen obtained his BSc in geology from the National Taiwan University and PhD in geophysics from the Massachusetts Institute of Technology. He is a professor of geophysics at the University of Illinois (Urbana-Champaign), serving as the Head of the Department of Geology since 2007. He also had joint appointments in the Department of Theoretical and Applied Mechanics, and the Department of Civil and Environmental Engineering. He coordinated multi-disciplinary, large-scale, international projects such as Hi-CLIMB and served in national/international advisory committees, including the Advisory Council of the Consortium for Materials Properties Research in Earth Sciences (COMPRES). His other researchinterests include 1) the interaction between the Earth's deep interior and plate tectonics, the salient results of which he summarized in the 2010 Francis Birch Lecture of the American Geophysical Union; 2) seismogenesis of both intra-plate and inter-plate earthquakes at all depths and tectonics settings; and 3) new methodology. Many of his articles and teaching materials (including some for field geology) are available at http://www.uiuc.edu/goto/pubs.

Shu-Huei Hung is an Associate Professor in the Department of Geosciences, National Taiwan University. Her research involves development andapplication of seismic tomography to the Earth's mantle. She obtained her Ph.D. from Brown University in 1998 and is one of the original developers of the “banana-doughnut” kernels for tomography. Lately she also developed a data-adaptive, multi-scale inversion scheme that is applicable to a wide variety of inverse problems.

Tai-Lin Tseng is an Assistant Professor in the Department of Geosciences, National Taiwan University. Her first research project was on the attenuation of inner core for her M.Sc. work in Geophysics at the National Central University of Taiwan. Subsequently, she worked at the Institute of Earth Sciences, Academia Sinica, Taiwan, and then obtained her PhD at the University of Illinois in 2007. She participated in many aspects of Project Hi-CLIMB to investigate the role of the mantle under Tibet during active continental collision.

Mike Brudzinski is an Associate Professor at Miami University, where he joined the Geology Department in 2005 after obtained a Ph.D. in Geophysics from the University of Illinois at Urbana-Champaign and an endowed postdoctoral fellowship at the University of Wisconsin-Madison. His overarching goal is to help people better understand the physical processes happening within the Earth, with a focus on subduction zones where tectonic plates converge. Mike carries the theme of natural hazards through his courses and provides research opportunities for students through seismic experiments in the Pacific Northwest and Mexico, investigating recently discovered forms of fault motion—episodic tremor and slip. He is working to further integrate his activities through a NSF CAREER award, which is expanding inquiry-based learning approach to new classes, undergraduate research experiences, and workshops for teaching environmental science in high schools.

Zhaohui Yang is a postdoctoral research associate in CIRES, University of Colorado, Boulder. She graduated from Peking University with a B.Sc. in Geophysics in 2000 and completed her PhD at University of Illinois at Urbana-Champaign in 2009. Her research interests focus on continental seismogenesis, rheology of continental lithosphere and lithospheric deformation.

Robert L. Nowack is a Professor of Geophysics in the Dept. of Earth and Atmos. Sciences at Purdue University in West Lafayette, Indiana. He is currently a Chief Editor for the Journal of Geophysical Research—Solid Earth. He was previously an Associate Editor for JGR-Solid Earth, Bull. Seism. Soc. Am., Journal of Geophysics and Engineering, and Studia Geophysica et Geodaetica. Since 2004, he has been a Fellow of the Institute of Physics (IOP). He received a BA in physics from Beloit College (Wisconsin), an MS in geophysics from Stanford University and a Ph.D. in geophysics from the Massachusetts Institute of Technology.